



Synthesis, characterization and biological activity of two Schiff base ligands and their nickel(II), copper(II), zinc(II) and cadmium(II) complexes derived from S-4-picolylidithiocarbamate and X-ray crystal structure of cadmium(II) complex derived from pyridine-2-carboxaldehyde



Teng-Jin Khoo^{a,*}, Mohammed Khaled bin Break^b, K.A. Crouse^c, M. Ibrahim M. Tahir^c, A.M. Ali^d, A.R. Cowley^e, D.J. Watkin^e, M.T.H. Tarafder^f

^a School of Pharmacy, Faculty of Science, University of Nottingham Malaysia Campus, Jalan Broga, 43500 Semenyih, Selangor, Malaysia

^b School of Chemical Sciences and Food Technology, Universiti Kebangsaan Malaysia, 43600 Bangi, Malaysia

^c Department of Chemistry, Faculty of Science, Universiti Putra Malaysia, Malaysia

^d Laboratory of Molecular and Cell Biology, Institute of BioScience, Universiti Putra Malaysia, 43400 Serdang, Selangor, Malaysia

^e Chemical Crystallography, Chemistry Research Laboratory, 12 Mansfield Road, Oxford University, OX1 3TA England, United Kingdom

^f Department of Chemistry, Rajshahi University, Rajshahi 6205, Bangladesh

ARTICLE INFO

Article history:

Received 1 November 2013

Received in revised form 23 December 2013

Accepted 3 January 2014

Available online 24 January 2014

Keywords:

S-4-Picolylidithiocarbamate

Synthesis

Characterization

Bioactivity of Schiff base ligands and complexes

X-ray crystal structure

ABSTRACT

A substituted dithiocarbamate moiety has been prepared using 4-picolylchloride hydrochloride to obtain S-4-picolylidithiocarbamate (S4PDTC) and its by-product (S4diPDTC). Two Schiff bases were synthesized by reacting S-4-picolylidithiocarbamate with pyridine-2-carboxaldehyde (Pc4PDTC) and 4-carboxybenzaldehyde (Cb4PDTC). Ni(II), Cu(II), Zn(II) and Cd(II) complexes of the Schiff bases were characterized by various physico-chemical and spectroscopic methods viz. CHNS elemental analyses, molar conductivity, IR, UV–Vis, ¹H and ¹³C NMR, mass spectrometry and magnetic susceptibility. X-ray crystallographic analysis has been carried out on the by-product and the Cd complex of the ligand derived from (Pc4PDTC). The ligands and their metal complexes were assayed *in vitro* for cytotoxic, antimicrobial and antioxidant activities. The Pc4PDTC Schiff base showed moderate cytotoxicity against human promyelocytic leukemic (HL60) cell line with a CD₅₀ value of 9 μg/cm³ while Cb4PDTC was inactive. Complexing Pc4PDTC with cadmium(II) and copper(II) enhanced its cytotoxicity against the human promyelocytic leukemic cell line (HL60) from moderately to highly active. S4PDTC showed marked antimicrobial activity against bacteria but was inactive towards fungi. Copper(II) and cadmium(II) complexes of the two Schiff bases showed clear inhibition zones for most of the fungi and bacteria tested. Antioxidant properties of Pc4PDTC and Cb4PDTC Schiff bases were comparable to the commercially available butylatedhydroxytoluene (BHT).

Crown Copyright © 2014 Published by Elsevier B.V. All rights reserved

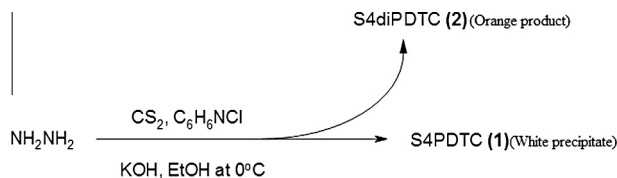
1. Introduction

The chemistry and the biological potential of Schiff base ligands derived from dithiocarbamates and their metal complexes have been investigated extensively [1–13]. Interest is still high as few have found their way into application as therapeutic drugs, health, skin care products and in paint dye manufacturing [1–3,14]. Most of the work previously has focused upon S-methyl and S-benzyl

dithiocarbamate Schiff bases and complexes, while S-picolylidithiocarbamate derivatives have started to be studied recently and have shown promising biological activities when investigated [15]. Therefore, this has led us to anticipate that a study of derivatives possessing pyridine will provide interesting results and may help develop an understanding of the biological activity of this class of compounds. We report herein the synthesis, separation and characterization of S-4-picolylidithiocarbamate (S4PDTC) (1) and the single crystal structure of its by-product (S4diPDTC) (2) together with two multidentate Schiff bases and their transition metal complexes. Moreover, their anti-microbial, cytotoxic and

* Corresponding author. Tel.: +60 389248213; fax: +60 389248018.

E-mail address: TengJin.Khoo@nottingham.edu.my (T.-J. Khoo).



Scheme 1. Reaction scheme for the synthesis of (1).

antioxidant activities have been evaluated and correlated with the newly elucidated structures. The expected structures for the two Schiff bases synthesized by reacting *S*-4-picolylthiocarbamate with 4-carboxybenzaldehyde (Cb4PDTC) (3) and pyridine-2-carboxaldehyde (Pc4PDTC) (4) are shown in Scheme 1.

2. Experimental

All chemicals and solvents were of analytical grade, and were used as supplied. 100% Hydrazine hydrate, carbon disulphide and potassium hydroxide were obtained from MERCK while $\text{Cd}(\text{CH}_3\text{COO})_2 \cdot 2\text{H}_2\text{O}$ and $\text{Cu}(\text{NO}_3)_2 \cdot 2.5\text{H}_2\text{O}$ were obtained from R&M MARKETING. 4-picolylchloride hydrochloride, pyridine-2-carboxaldehyde and 4-carboxybenzaldehyde were obtained from SIGMA-ALDRICH while absolute ethanol, $\text{NiCl}_2 \cdot 6\text{H}_2\text{O}$, and ZnCl_2 were obtained from FRIENDEMANN SCHMIDT.

2.1. Preparation of (1) and its Schiff bases

100% Hydrazine hydrate (10 g, 0.31 mol) was added to KOH (11.4 g, 0.20 mol) in 90% EtOH (70 ml) and the mixture cooled to 0°C in an ice bath. CS_2 (15.2 g, 0.20 mol) was added dropwise with constant stirring (880 rpm) for 1 h. During this time two layers formed and the lower layer (light brown) was separated then dissolved in cold 40% EtOH (60 ml). The ethanolic solution was kept in an ice bath while 4-picolylchloride hydrochloride (32 g, 0.2 mol) dissolved in 80% MeOH was added dropwise with vigorous stirring (1100 rpm). The yellowish precipitate which formed after ~ 2 h was filtered and dried over anhydrous silica gel and was later dissolved in MeOH to give a white precipitate and dark-orange solution. The white precipitate was filtered off, dried and

characterized. The dark-orange solution filtrate was rotavaporated. The crude formed was rinsed and washed with cold MeOH to give an orange solid which was dried and characterized. The white precipitate that did not dissolve in MeOH was characterized to be (1) and the latter was (2).

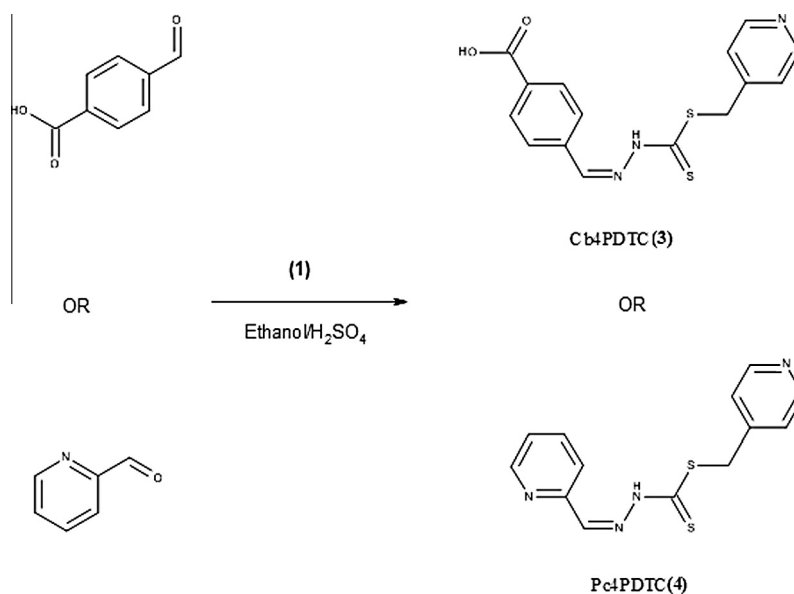
Schiff bases were prepared by adding a solution of (1) (0.1 mol) in absolute ethanol (40 cm^3) to an equimolar amount of the aldehyde dissolved in 50 cm^3 of the same solvent in the presence of 1–2 drops of sulfuric acid. The mixture was heated on a steam bath for 10 min and then cooled to room temperature until the Schiff bases precipitated. Products were washed with cold ethanol and dried *in vacuo* over silica gel. The yield was determined and the melting point recorded. Schemes 1 and 2 illustrate the synthesis procedures for the compounds.

2.2. Preparation of metal complexes

Schiff bases (7.6 mmol) prepared as outlined above were dissolved in ethanol (50 cm^3). These solutions were combined with solutions containing a stoichiometric amount of metal salt in the same solvent ($\sim 50\text{ cm}^3$). The mixtures were heated to 100°C for 5 min and then the volume of each was reduced by $\sim 40\%$. Products precipitated were isolated, and dried in a vacuum desiccator over P_2O_5 . Attempts to synthesize the $\text{Ni}(\text{II})$ complex of (4) were unsuccessful.

2.3. Physical measurements

The analyses for carbon, hydrogen, nitrogen and sulfur were carried out using a LECO CHNS-932 analyzer. The IR spectra (KBr pellets) were recorded ($4000\text{--}400\text{ cm}^{-1}$) using a Perkin Elmer FTIR 1750X spectrophotometer. The molar conductance of a 10^{-3} M solution of each metal complex in DMSO was measured at 29°C using a Jenway 4310 conductivity meter and a dip-type cell with a platinized electrode. Melting points were determined using an Electrothermal digital melting point apparatus while the UV–Vis spectra were recorded on a Shimadzu UV-2501 PC spectrophotometer ($800\text{--}200\text{ nm}$) in DMSO solution. Magnetic susceptibility was determined using a Sherwood Scientific MSB-AUTO Magnetic Susceptibility Balance at room temperature. ^1H and ^{13}C spectra were obtained using a 400 MHz JEOL JNM-ECA instrument. Mass spectra



Scheme 2. Reaction scheme for synthesis of the Schiff base ligands (3) and (4).

were obtained using a SHIMADZU GCMS QP5050A DIMS with Electron Ionization technique.

2.4. X-ray crystal structure determination

Suitable quality crystal were mounted on glass fibers using perfluoropolyether oil and cooled rapidly to 150 K in a stream of cold N₂ using an Oxford Cryosystems CRYOSTREAM unit. Diffraction data were measured using an Enraf–Nonius KappaCCD diffractometer (graphite monochromated Mo K α radiation, $\lambda = 0.71073$ Å). Intensity data were processed using the DENZO-SMN package [16]. The structures were solved using the direct-methods program SIR92 [17], which located all non-hydrogen atoms. Subsequent full-matrix least-squares refinement on F was carried out using the CRYSTALS program suite [18].

Coordinates and anisotropic thermal parameters of all non-hydrogen atoms were refined. All other hydrogen atoms were positioned geometrically after each cycle of refinement. Important crystallographic data for the elucidated structures are presented in Table 1.

2.5. Biological activity

2.5.1. Cytotoxicity

The CEM-SS (Human T-lymphoblastic leukemic) and HL60 (Human promyelocytic leukemic) cell lines were obtained from the National Cancer Institute, USA. The cells were cultured in RPMI-1640 (Sigma) medium supplemented with 10% fetal calf serum. Cytotoxicity was determined using the microtitration of 3-(4,5-dimethylthiazol-2-yl)-2,5-diphenyltetrazolium bromide (MTT) assay (Sigma, USA) as reported by Mosmann [19]. Cytotoxicity was expressed as CD₅₀, i.e. the concentration that reduced the absorbance of treated cells by 50% with reference to the control (untreated cells).

Table 1
Crystallographic data and structure refinement details.

	(2)	(5)
Empirical weight	C ₁₅ H ₁₉ N ₄ O ₁ S ₂	C ₂₀ H _{18.67} Cd _{1.33} Cl _{1.33} N _{5.33} O _{0.67} S _{2.67}
Formula weight	335.47	627.05
T	150	150
Crystal class	triclinic	monoclinic
Space group	$P\bar{1}$	$P2_1/n$
<i>Unit cell dimensions</i>		
a (Å)	4.5627(2)	8.1716(2)
b (Å)	10.4137(3)	20.8073(4)
c (Å)	17.2731(7)	10.7152(3)
α (°)	83.9493(13)	90
β (°)	84.1499(14)	101.7141(12)
γ (°)	78.1442(15)	90
Volume (Å ³)	796.02(5)	1783.95(8)
Z	2	3
ρ_{calc} (g cm ⁻³)	1.40	1.751
Radiation type	Mo K α	Mo K α
Wavelength (Å)	0.71073	0.71073
Crystal size (mm)	0.01 × 0.01 × 0.01	0.10 × 0.10 × 0.10
θ (°)	5–27	5–27
Reflections measured/independent (R_{int})	6467/3554 (0.0002)	7254/4003 (0.017)
θ_{max}	27.42	27.5
Limiting indices	$-5 \leq h \leq 5, 13 \leq k \leq 13, -22 \leq l \leq 22$	$-10 \leq h \leq 10, -27 \leq k \leq 26, -13 \leq l \leq 13$
Refinement on	F	F
R -factor	0.057	0.032
R_w -factor	0.058	0.039
Goodness of fit (GOF) on F	1.038	1.00
Minimum and maximum residual electron density (e Å ⁻³)	-0.65 and 0.75	-0.68 and 1.15
Reflections used	2687	3180
$\sigma(I)$ limit	3.00	3.00
Number of parameters	200	226

2.5.2. Antimicrobial assay

Antimicrobial activity of each sample was qualitatively determined by a modified disc diffusion method as previously reported [12]. Compounds that showed positive (>15 mm) antimicrobial activities with the disc diffusion assay were subjected to the broth dilution method for the quantitative measurement of microbio-static (inhibitory) activity as described by Hufford and Clark [20]. The lowest concentration that completely inhibited visible microbial growth was recorded as the minimum inhibitory concentration (MIC, $\mu\text{g}/\text{cm}^3$). The pathogenic microbials used were *Methicillin resistant staphylococcus* (MRSA), *Bacillus subtilis wild type* (B29), *Subtilis mutant* (mutant defective DNA repair-B28), *Pseudomonas aeruginosa* (60690), *Candida albicans* (C.A.), *Aspergillus ochraceous* (398), *Saccaromyces ceciricae* (20341) and *Candida lypolytica* (2075).

2.5.3. Antioxidant assay

Antioxidant assays were carried out using the ferric thiocyanate (FTC) method as previously reported by Kikuzaki and Nakatami [21]. A mixture of 0.002 g of sample in 99.5% ethanol (4 cm³), 4.1 cm³ of 2.51% linoleic acid in 99.5% ethanol, 8 cm³ of 0.05 M phosphate buffer (pH 7) and 3.9 cm³ of H₂O in a vial (diam. = 38 mm, $h = 75$ mm) with screw cap was placed in a dark oven at 40 °C. To 0.1 cm³ of this solution was added 9.7 cm³ ethanol (75%) and 0.1 cm³ NH₄CNS (30%). Precisely 3 min. after the initial addition of 0.1 cm³ of 2×10^{-2} M FeCl₂ in 3.5% HCl to the reaction mixture, the red absorbance was measured at 500 nm. Subsequently, readings were taken at 24 h intervals until the absorbance of the control reached its maximum.

3. Results and discussion

3.1. Physical properties and analytical data of Schiff base ligands and their complexes

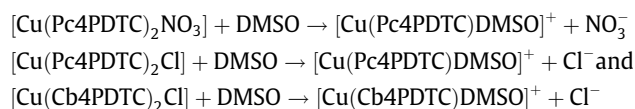
The physical properties and analytical data results have been summarized in Table 2. Results of the CHNS elemental analyses

Table 2
Analytical data and physical properties of the Schiff bases and their complexes.

Compound	Color	m.p (°C)	Found (Calcd.) (%)				Molar conductance ($\Omega^{-1} \text{ cm}^2 \text{ mol}^{-1}$)
			C	H	N	S	
(1)	beige	184–86	57.5 (42.2)	5.2 (4.5)	11.4 (21.1)	26.3 (32.2)	–
(2)	orange						
(3)	pale orange	320	55.5 (54.4)	4.4 (4.0)	12.4 (12.7)	19.9 (19.3)	–
(4)	pale yellow	189	53.9 (54.2)	4.5 (4.2)	19.2 (19.4)	22.1 (22.2)	–
[Cd(Pc4PDTC) ₂] (5)	dark yellow	~250d	39.4 (39.0)	3.2 (3.2)	12.6 (12.1)	13.8 (13.9)	non-electrolyte
[Cu(Pc4PDTC) ₂ Cl] (6)	dark green	182	37.4 (38.3)	2.8 (3.1)	17.1 (14.0)	14.9 (15.7)	59
[Cu(Pc4PDTC) ₂ NO ₃] (7)	green	174	37.5 (37.5)	2.7 (2.9)	17.1 (16.8)	14.9 (15.4)	63
[Zn(Pc4PDTC) ₂] (8)	orange	~260d	42.7 (43.4)	3.6 (3.6)	13.6 (13.5)	15.1 (15.4)	non-electrolyte
[Cd(Cb4PDTC) ₂] (9)	pale yellow	>270d	41.9 (40.6)	3.4 (3.2)	9.5 (8.4)	12.9 (12.7)	non-electrolyte
[Cu(Cb4PDTC) ₂ Cl] (10)	light green	278	41.1 (41.9)	3.4 (3.0)	9.5 (9.8)	16.1 (14.9)	41
[Ni(Cb4PDTC) ₂] (11)	dark brown	>235d	45.0 (45.5)	3.9 (3.6)	10.5 (9.4)	16.9 (14.3)	10
[Zn(Cb4PDTC) ₂] (12)	light yellow	>300d	43.7 (44.8)	3.4 (3.5)	9.1 (9.2)	15.5 (14.1)	non-electrolyte

Notes: d = decompose.

for both Schiff base ligands were in agreement with calculated values and the case was similar with their complexes. Molar conductance studies have revealed that (7), (6) and (10) are 1:1 electrolytes having molar conductivities of 63, 59 and 41 $\Omega^{-1} \text{ cm}^2 \text{ mol}^{-1}$ in DMSO, presumably due to solvation according to the following equations:



All the complexes dissolve readily only in donor solvents such as DMSO and DMF. The chloride ion that has been included in the formulas for Cu complexes might have come from 4-picolychloride hydrochloride. The molar conductivity value for (11) has been found to be very low to account for any dissociation of the complexes in DMSO indicating its non-electrolytic nature. Elemental analyses data suggest a 2:1 ligand to metal ratio for the complexes, and all of these data have been used to suggest formulas for the complexes.

3.2. 2.IR spectral analysis

The IR spectra of the compounds have been tabulated in Table 3. IR spectrum for (1) displays bands at 3234, 1608, 1142 and 1072 cm^{-1} assigned to $\nu(\text{NH})$, $\nu(\text{NH}_2)$, $\nu(\text{C}=\text{S})$ and $\nu(\text{N}=\text{N})$, respectively. The absorption peaks at 666 and 756 cm^{-1} indicate mono-substitution of the pyridine ring.

Characterization via IR indicated that the Schiff bases formed were indeed obtained as proposed. The solid state IR spectra of both free Schiff bases display bands for $\nu(\text{C}=\text{S})$, $\nu(\text{C}=\text{N})$, $\nu(\text{NH})$

and $\nu(\text{N}=\text{N})$ but do not exhibit $\nu(\text{S}=\text{H})$ at ca. 2700 cm^{-1} . All these are characteristic of an unprotonated Schiff base in its thione form, as it is well documented [6–13] that this type of dithiocarbamate moiety can display thione-thiol tautomerism in solution (Fig. 1). The band indicating ortho-substitution of pyridine appears at 628 cm^{-1} and is as expected for (4). (3) also displays the characteristic carboxylic acid functionality with carboxylic $\nu(\text{O}=\text{H})$ band in the 3100–3550 cm^{-1} range and $\nu(\text{C}=\text{O})$ at 1688 cm^{-1} while the para-substitution of the benzene ring has been confirmed by an absorption peak at 768 cm^{-1} . As for the metal complexes, the strong bands assigned to $\nu(\text{NH})$ at 3234 and 2920–2972 cm^{-1} for (1) and its Schiff bases were lost in all the metal complexes. This deprotonation of the nitrogen atom is believed to be due to the tautomerism phenomenon whereby the ligands exist in their thiol forms within the complex. The red shift of azomethine $\nu(\text{C}=\text{N})$ stretching band and the loss of $\nu(\text{C}=\text{S})$ bands in all the complexes, indicate coordination of the ligands with metal ions via the azomethine nitrogen and thiolato group. The formation of a metal–nitrogen ($\beta\text{-N}$) bond results in lowering of $\text{C}=\text{N}$ bond order thus decreasing the $\nu(\text{C}=\text{N})$ band frequencies, however the band frequencies were found to increase after coordination and this might be due to decrease in repulsion between the nitrogen lone pair of electrons and the nearby electrons as a result of participation of the nitrogen electrons in coordination with the metal ion [12]. Complexes of (4) showed no major shift of the para substituted pyridine band at 775 cm^{-1} , however the ortho substituted out-of-plane and in-plane pyridine bands showed generally positive shifts which might indicate that the ligand undergoes coordination with the metal ions via the nitrogen atom of the pyridine ring. Furthermore, complexes of (3) showed positive shifts in the bands for para pyridine indicating their involvement in chelation,

Table 3
Infrared spectral data (band maxima).

Compound	Infrared Absorption Bands (frequency, cm^{-1})							Pyridine bands
	$\nu(\text{C}=\text{S})$	$\nu(\text{C}=\text{N})$	$\nu(\text{O}=\text{H})$	$\nu(\text{NH})$	$\nu(\text{N}=\text{N})$	$\nu(\text{NH}_2)$	$\nu(\text{Ar}-\text{COOH})$	
(1)	1142	*	*	3234	1072	1608	*	756 (para)
(3)	1116	1608	3438	2972	1070	–	1688	768 (para)
(4)	1148	1606	*	2920	1044	–	*	406(ip), 628(op) (ortho)
(5)	–	1616	*	–	1064	–	*	410(ip), 618(op) (ortho)
(6)	–	1610	*	–	1070	–	*	421(ip), 648(op) (ortho)
(7)	–	1612	*	–	1070	–	*	421(ip), 649(op) (ortho)
(8)	–	1616	*	–	1068	–	*	414(ip), 634(op) (ortho)
(9)	–	1608	3424	–	1068	–	1688	782
(10)	–	1636	3434	–	1042	–	1694	764
(11)	–	1610	3425	–	1071	–	1690	778
(12)	–	1608	3436	–	1069	–	1689	780

– = Lost, “ip” = in-plane, * = not present, “op” = out-of-plane.

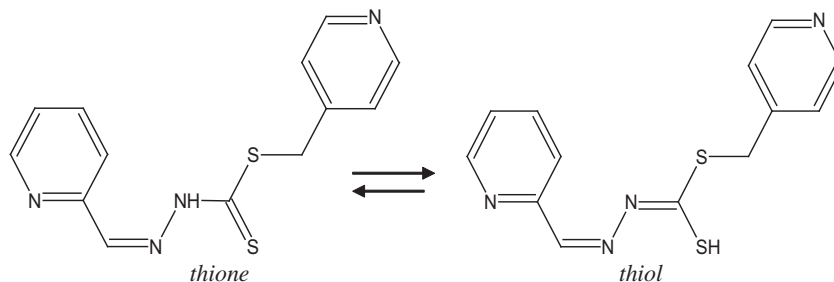


Fig. 1. Thione and thiol tautomers of pyridine-2-carboxaldehyde Schiff base (4).

while the lack of any shifts in the bands representing the carboxylate functionality present in the complexes indicates that the carboxylate group is not involved in any coordination with the metal ions.

3.3. Mass spectrometry, UV-Vis and magnetic susceptibility

Mass spectral data revealed that the synthesized products were obtained as expected. MS characterization confirmed the presence of (1) and its by-product (2) through the highest m/z at 199 for (1) and highest m/z at 288 for (2). Fragment of (1) at m/z 92 points to the presence of methylpyridine while m/z 107 represents the dithiocarbamate moiety. In (2), the fragment m/z 105 indicates the presence of aminomethylpyridine, a clear indication of the formation of the ligand.

Furthermore, the mass spectral data for the Schiff base ligands confirmed the presence of these compounds as expected, whereby the mass spectra obtained for (3) and (4) showed the highest m/z at 329 for the former and m/z 288 for the latter. Characteristic fragments appearing in the spectrum of each Schiff base are, m/z 105 representing the dithiocarbamate moiety and m/z 92 indicating methyl pyridine. The peak at m/z 130 (methylbenzylcarboxyl) appearing in the spectrum of (3) and m/z 78 (pyridine) in that of (4), indicate the presence of the expected functionality in each molecule.

The electronic spectral data recorded in DMSO and magnetic moments of the complexes are given in Table 4. The absorptions with wavelengths less than 350 nm are mostly due to ligand centered transitions of aromatic electrons ($\pi \rightarrow \pi^*$) in addition to non-bonding electrons ($n \rightarrow \pi^*$) present in the nitrogen atom of the azomethine group in the Schiff base complexes. The bands at around 400 nm might be assigned to electron transitions from the $p\pi$ orbitals of the donor atoms to the d -orbitals of the metal, while the bands that are around 650 nm can be assigned to $d-d$ transitions in the complexes [22]. The band referring to $d-d$ transitions for Cu complexes can be assigned to ${}^2E_g \rightarrow {}^2T_{2g}$ transitions and indicates a Jahn–Teller distorted octahedral arrangement [23]. It is possible that the band at 400 nm for the Ni complex is

caused by ${}^3A_{2g}(F) \rightarrow {}^3T_{1g}(P)$ transitions and might indicate an octahedral arrangement [22,23].

Magnetic susceptibility data have revealed that (8) was found to be diamagnetic at room temperature in accordance with a d^{10} configuration while (11) is paramagnetic with a μ_{eff} value of 1.52 B.M which appears to deviate from spin only values as it falls within the range of (0–2.8) [24]. Previous studies on the magnetic susceptibilities of Ni complexes have shown that some of these complexes might exhibit such values, and the reason has been attributed to spin state isomerism, presence of more than one stereochemistry for the complex in the unit cell or due to interactions between solvent molecules and complex [24]. The μ_{eff} values of Cu complexes seem to be higher than the normal values of (1.7–1.8) and that could be due to the presence of interactions between ethanol solvent molecules and the Cu complexes or due to the presence of ferromagnetic interactions [25–27].

3.4. ${}^1\text{H}$ and ${}^{13}\text{C}$ NMR

The clearest characterization of the synthesized compounds can be seen from the ${}^1\text{H}$ NMR and ${}^{13}\text{C}$ NMR spectra in DMSO- d_6 at 18 °C, where the ${}^1\text{H}$ NMR spectrum of (1) showed the following signals: the pyridine ring protons appear as doublets at 8.48 ppm ($J=4.6$ Hz) and 7.38 ppm ($J=6.0$ Hz) while the singlet at 4.33 ppm is assigned to $-\text{SCH}_2-$ protons. Spectrum of ${}^{13}\text{C}$ NMR showed the presence of single pyridine ring at 150.3 and 124.4 ppm for the four carbons.

In both the ${}^1\text{H}$ NMR and ${}^{13}\text{C}$ NMR of (2), the presence of two pyridine rings is very clear as indicated by chemical shift at 7.28 and 8.60 ppm (shift for *ortho*-pyridine protons) for the hydrogens in the pyridine attached to thiolato group while the shift at 8.02 and 8.83 ppm (*ortho*-pyridine protons) points to hydrogen in the other pyridine. Carbon shifts are indicated at 124.4, 150.3, 124.1 and 149.9 ppm corresponding to the similar positions.

${}^1\text{H}$ NMR spectra of both Schiff bases were determined in DMSO- d_6 : (3): δ 7.25(2H, d), δ 7.08(1H, s), δ 6.78(2H, d), δ 6.57(2H, d), δ 6.20(2H, d) and δ 3.30(2H, s) while (4): δ 7.70(2H, d), δ 7.60(2H, d), δ 7.40(1H, s), δ 7.00(2H, d), δ 6.60(2H, d) and δ 3.70(2H, s). These data are in line with expectations in each case.

3.5. Crystal structure of (2)

ORTEP diagram of (2) molecule with atom numbering scheme is shown in Fig. 2, while significant bond lengths and angles have been summarized in Table 5. The molecule is L-shaped and is mostly planar except for the pyridine ring attached to the thiolato group which is twisted around 79.08° relative to the rest of the molecule. The fact that (C7–S2) is shorter than the single bond (C7–S1), with bond lengths of 1.658 and 1.752 Å respectively, proves that the former contains a double bond and that the molecule exists in its thione tautomer. Moreover, the bond C7–N2 has a length of 1.351 Å whereas C8–N3 has a bond length of 1.284 Å

Table 4
UV-Vis and magnetic susceptibility.

Compounds	UV-Vis Spectra ^a (λ_{max} , nm)	μ_{eff} (B.M.)
(5)	259 (4.1), 322 (4.3), 381 (4.2)	diamag.
(6)	333 (4.5), 409 (4.2), 654 (2.5)	2.78
(7)	331 (4.5), 408 (4.1), 650 (4.0)	2.93
(8)	326 (2.7), 393 (2.7)	diamag.
(9)	300 (4.4), 350 (4.7)	diamag.
(10)	332 (3.9), 347 (3.7)	3.0
(11)	346 (4.4), 364 (4.3), 400 (3.8)	1.52
(12)	304 (4.2), 320 (4.2), 333 (4.2) 3.92	3.92

^a Log ϵ (L cm⁻¹ mole⁻¹) are given in parentheses.

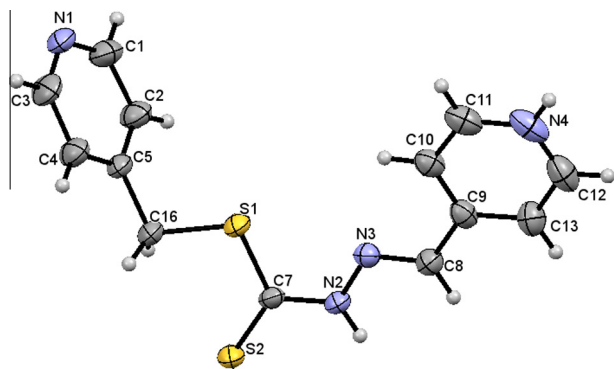


Fig. 2. ORTEP diagram of (2) (at 50% probability displacement ellipsoids) with atomic numbering scheme. Ethanol solvent molecule has been obscured for clarity.

Table 5
Selected geometry parameters of (2) (Å, °).

C1–N1	1.339 (5)	C8–N3	1.284 (4)
C14–O6	1.615 (19)	N2–N3	1.362 (4)
C7–S1	1.752 (3)	C7–S2	1.658 (3)
C2–C1–N1	122.8 (4)	C16–S1–C7	101.94 (15)
S1–C7–N2	112.9 (2)	C7–N2–N3	118.6 (2)
C15–C14–O6	169.1 (16)	C14–O6–H5	155.4

Table 6
Hydrogen bond interactions of (2) (Å, °).

D–H...A	D–H	H...A	D...A	D–H...A
N2–H7...N1 ⁱ	0.86	1.96	2.800 (4)	164
N4–H20...N4 ⁱⁱ	0.83	1.87	2.703 (5)	178
C4–H4...S2 ⁱⁱⁱ	0.93	2.87	3.782 (4)	165
C15–H18...O6 ^{iv}	0.96	1.88	2.804 (16)	159
C16–H21...S2 (Intramolecular)	0.97	2.74	3.127 (3)	105

Symmetry codes: (i) $x, y + 1, z$; (ii) $-x + 4, -y - 1, -z + 1$; (iii) $-x + 2, -y - 1, -z$; (iv) $x + 1, y, z$.

which is shorter than the former indicating that the latter possesses a double-bond character and belongs to the imine group. The molecule crystallizes in the conformer in which the thione

sulfur is in a *trans* position with the pyridine ring attached to the imine group while the pyridine rings are *cis* to each other, across the C7–N2 bond.

Analysis of any interactions between the molecules in the structure revealed the presence of hydrogen bond interactions (Table 6). The nitrogen at the two pyridine rings, lay good 2-dimensional hydrogen bond linkages in the molecular packing (Fig. 3). The distance between layers in the molecular packing varies from 4.563 Å (maximum) in some areas to a minimum value of 3.363 Å in other regions and such distances are enough to accommodate an ethanolic solvent molecule, which in this case, is an ethanolic molecule that is disordered.

Overall, the structure seems very similar to (4) except that both pyridine rings in this by-product are at the *para* position while (4) has one of the pyridine rings substitution in *ortho* position.

3.6. Crystal structure of (5)

The molecular structure of (5) along with the atomic numbering scheme is shown in Fig. 4, while significant bond lengths and angles have been summarized in Table 7. The compound crystallizes with a distorted ethanolic molecule and is a dinuclear complex containing two cadmium ions bridged by two chlorine atoms. The chloride ions are thought to have come from trace amounts of 4-picolylchloride hydrochloride that was initially used to synthesize the complex. The asymmetric unit comprises of half the molecule while the other half is related *via* a centre of inversion situated in the Cd1–Cl1–Cd1–Cl1 ring. The distance between the two cadmium ions is 3.906 Å while each cadmium ion is coordinated to six atoms (N1, N4, N3, S2, Cl1, Cl1) in a distorted octahedral geometry. This form of geometry was further proven by the following bond angles of (N1–Cd1–Cl1 = 163.93°), (S2–Cd1–N4 = 144.01°) and (N3–Cd1–Cl1 = 170.78°) which indicate that the ligands are nearly orthogonal to each other thus forming a distorted octahedral geometry. Coordination polymer is formed by N1–Cd coordination, moreover, the ligand coordinates in a facial fashion.

The coordination bonds between each of the Cd ions with the Schiff base ligands result in the formation of fused rings around each Cd ion; (Cd1–S2–C7–N2–N3) and (N3–C8–C10–N4–Cd1), furthermore, another cyclic structure is formed from the coordination of Cd with Cl. The 5-membered ring (Cd1–S2–C7–N2–N3) possesses an envelope conformation on Cd 1 with puckering

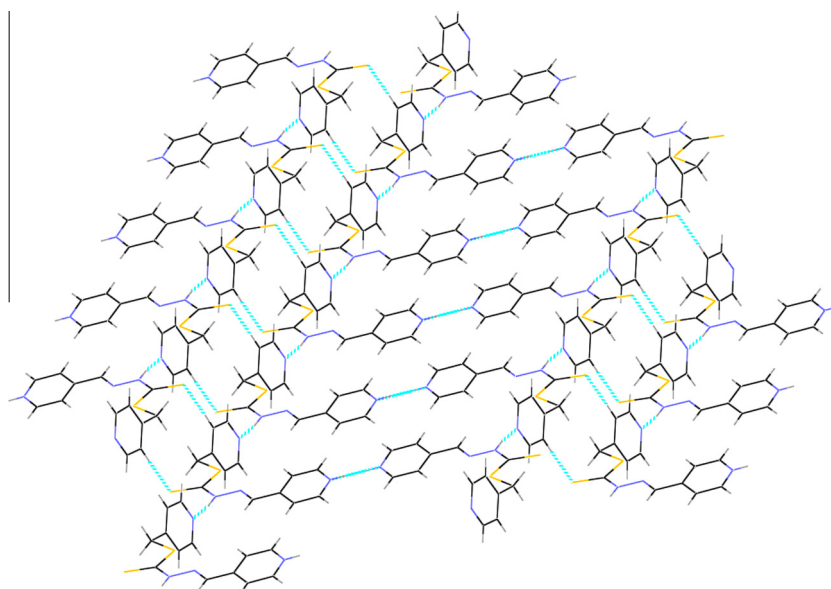


Fig. 3. 2-Dimensional hydrogen bond network of (2) molecules.

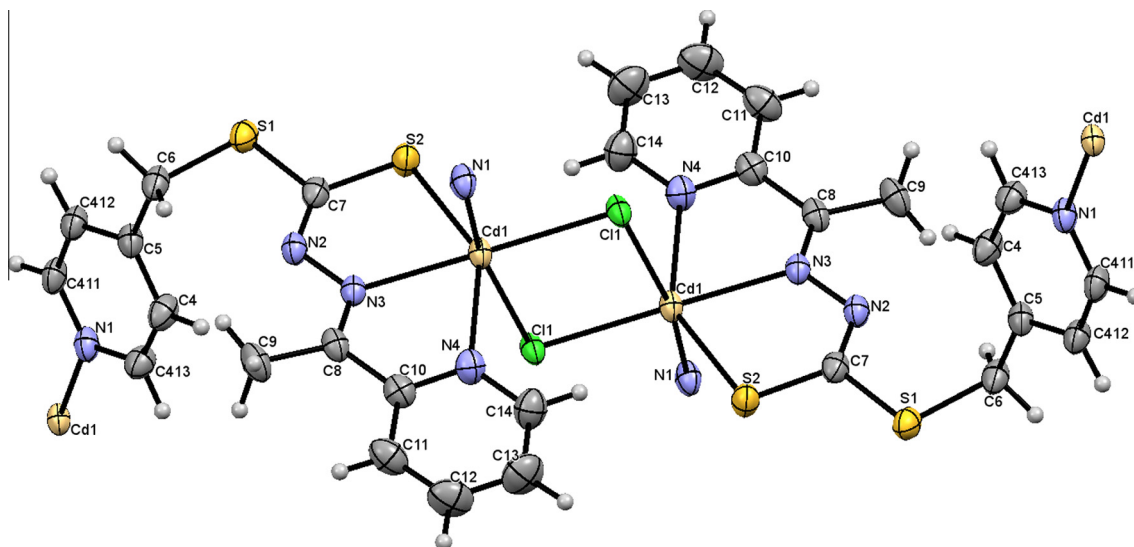


Fig. 4. ORTEP diagram of (5) (at 50% probability displacement ellipsoids) with atomic numbering scheme. Ethanol solvent molecule has been obscured for clarity.

Table 7

Selected geometry parameters of $[Cd(Pc4PDTC)CH_3COO]$ (\AA , $^\circ$).

C1–Cd1	2.7055 (7)	S2–Cd1	2.5742 (8)
C413–N1	1.348 (4)	N1–Cd1	2.441 (3)
C7–S1	1.758 (3)	N4–Cd1	2.365 (3)
C8–N3	1.292 (4)		
Cd1–C11–Cd1	95.99 (2)	C7–S2–Cd1	96.02 (11)
C412–C411–N1	123.6 (3)	Cd1–N1–C413	124.7 (2)
C5–C6–S1	111.3 (2)	N2–N3–Cd1	121.76 (19)
S1–C7–S2	111.22 (19)	N1–Cd1–Cl1	163.93 (7)
S1–C7–N2	117.6 (2)	Cl1–Cd1–N4	82.96 (7)

Table 8

Hydrogen bond interactions of (5) (\AA , $^\circ$).

Cg is the centroid of the ring (Cd1–N3–C8–C10–N4)				
D–H...A	D–H	H...A	D...A	D–H...A
C4–H4...N2 (Intramolecular)	0.93	2.62	3.316 (4)	132
C6–H6...N2 (Intramolecular)	0.97	2.40	2.872 (4)	110
C9–H8...N2 (Intramolecular)	0.96	2.33	2.766 (5)	106
C6–H5...C11 ⁱ	0.97	2.68	3.639 (3)	169
C413–H3...Cg ⁱⁱ	0.94	2.65	3.177 (3)	116

Symmetry codes: (i) $-x + 1/2, y + 1/2, -z + 1/2$; (ii) $x - 1/2, -y + 1/2, z + 1/2$.

parameters; $Q = 0.0988 (18) \text{\AA}$, $\varphi = 174.6 (16)^\circ$. Q stands for the puckering amplitude and assesses the extent of deviation of a certain ring from planarity while φ stands for the pseudorotation phase angle. The puckered (Cd1–S2–C7–N2–N3) atoms possess deviations from planarity of $-0.0620(10)$, $0.0467(12)$, $-0.014(3)$, $-0.025(3)$, $0.054(2) \text{\AA}$, respectively.

The other fused 5-membered ring (Cd1–N3–C8–C10–N4) exhibits a twisted conformation on Cd1–N3 bond with puckering parameters; $Q = 0.121(3) \text{\AA}$, $\varphi = 204.9(15)^\circ$. The puckered (Cd1–N3–C8–C10–N4) atoms show deviations from planarity of $-0.0693(12)$, $0.075(3)$, $-0.052(3)$, $0.009(3)$, $0.037(3) \text{\AA}$, respectively.

The 4-membered ring formed from the coordination of Cd ions with chlorine atoms is a perfect square planar with an r.m.s deviation of 0.000\AA .

The Schiff base ligand is essentially planar with an r.m.s deviation of 0.093\AA , except for the 4-pyridine ring of the dithiocarbazate moiety which is nearly perpendicular to the rest of the Schiff base ligand with a torsion angle (C5–C6–S1–C7) of 91.67° . The similarity of the (C7–S2) bond length of 1.739\AA to that of the single bond (C7–S1) which has a bond length of 1.758\AA , shows that the ligand coordinates with the metal ion *via* its thiol tautomer. Moreover, the shorter (C8–N3) bond length of 1.292\AA relative to that of the (C7–N2) indicates the presence of a double-bonded imine group. The (C–N) and (C–S) bond lengths are similar to that of

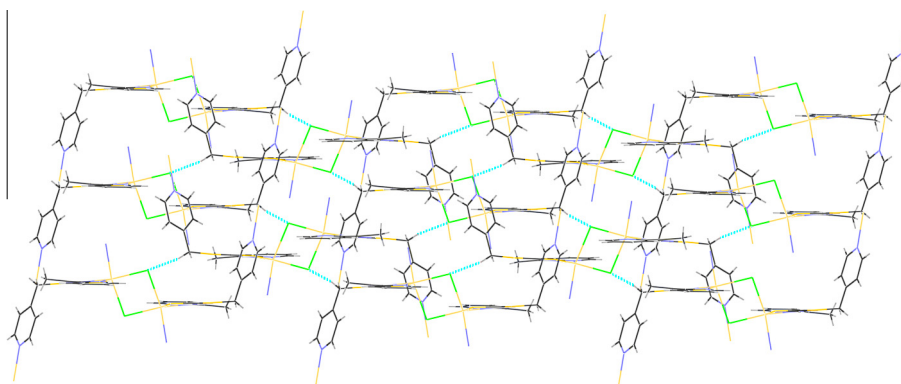


Fig. 5. 1-dimensional hydrogen bond network of (5) molecules.

previously reported related structures [28,29], which might indicate that such bond lengths are typical of Schiff base ligands and complexes derived from dithiocarbazates. The ring formed by Cd and Cl form an angle of $97.91(4)^\circ$ with the plane defined by the chelate system (S2, Cd1, N4, C10, C8, N3, N2, N7).

Analysis of interactions between molecules of the complex revealed the absence of significant π - π interactions. However, inter- and intramolecular hydrogen bonding interactions exist between the molecules of the complex, as well as C-H... π interactions (Table 8). The C6-H5...Cl1 intermolecular hydrogen bond links the molecules of the crystal to form one-dimensional polymeric chains (Fig. 5).

Table 9

Results for screening against colon cancer cells (HT-29) and human promyelocytic leukemic cells (HL60).

Compounds	CD ₅₀ ($\mu\text{g}/\text{cm}^3$)	
	HT-29	HL 60
(1)	10.5	13.2
(4)	0.7	9.0
(5)	0.8	1.20
(6)	1.0	1.50
(7)	0.4	1.70
(8)	16.8	ict
(3)	22.0	ict
(9)	23.4	6.40
(10)	5.5	ict
(11)	ict	ict
(12)	N.A	ict
Standard:		
Doxorubicin	6.0	N.A
Tamoxifen	36.00	N.A

Notes: N.A = not available, ict = inactive.

CD₅₀ ($\mu\text{g}/\text{cm}^3$) = the concentration to reduce growth of malignant cells by 50%.

CD₅₀ < 5 $\mu\text{g}/\text{cm}^3$ are very active, between 5 and 10 $\mu\text{g}/\text{cm}^3$ are moderate, 10–20 $\mu\text{g}/\text{cm}^3$ are weak while >20 $\mu\text{g}/\text{cm}^3$ are inactive.

3.7. Cytotoxic activities

The results of cytotoxicity screening are given in Table 9. (4) is moderately active against HL 60 cell lines while (3) is inactive in its free ligand form. However, the cytotoxicity of (4) towards human promyelocytic leukemic cells (HL 60) increases upon formation of the complexes (5), (6) and (7) to the highly active region with CD₅₀ values of 1.20, 1.50 and 1.70 $\mu\text{g}/\text{cm}^3$ respectively. Such concentrations are generally considered to be in the therapeutically useful range and are therefore worthy of further study. The Schiff base containing two pyridine rings, (4), was highly active against HT-29 with CD₅₀ of 0.7 $\mu\text{g}/\text{ml}$ while (3) was found to be inactive towards both cell lines assayed. This difference can possibly be attributed to the presence of the lone pair donor electrons on the nitrogen in (4) as these electrons can attack the DNA of tumour cells. In contrast, the comparative stability of the carboxylic functionality in (3) might have given rise to its inactivity against both cell lines. The cadmium(II) and two copper(II) complexes of (4) are also highly active against HT-29 and HL 60 while it is interesting to note that among the complexes of (3) studied in this work, only (10) is active against HT-29. Our previous findings have also shown [12,13,29,15] that chelation of Schiff bases with cadmium(II) metal ion enhanced the activity significantly, however it can be observed that Zn(II) complexes are not active although Zn(II) is too a d¹⁰ metal.

3.8. Antimicrobial activity

Qualitative and quantitative antimicrobial test results are presented in Tables 10 and 11. The entire range of compounds was evaluated against four types of fungi and bacteria. The results indicated that only copper(II) and cadmium(II) complexes are active and were thus the only ones reported. (9) and (10) are antimicrobial but are not active against cancer cell lines. (9) is selectively active against *candida albicans* (C.A.) with an MIC value of 781 $\mu\text{g}/\text{ml}$, making it potentially useful as a specific drug against

Table 10

Qualitative antimicrobial assay results^a/mm.

Compounds	2075	CA	398	20341	B28	B29	MRSA	60690	60691
(1)	–	14	14	14	~	27	28	23	~
(4)	–	–	–	–	~	10	7	–	~
(5)	~	11	–	15	–	–	–	10	~
(6)	~	15	20	12	14	14	16	~	17
(7)	~	17	25	15	15	14	17	~	17
(3)	–	–	–	–	–	12	10	–	~
(9)	~	15	–	12	8	7	–	~	–
(10)	~	14	32	11	15	11	16	~	9
Streptomycin (antifungal control)	~	~	~	~	30	30	31	30	~
Nystatin (antifungal control)	27	21	25	24	~	~	~	~	~

Notes: – = Tested compound inactive, ~ = not tested.

^a Inhibition diameters of 15 mm and above indicate that the compound is active.

Table 11

Quantitative antimicrobial assay results/MIC ($\mu\text{g}/\text{ml}$).

Compound	CA	398	20341	B28	B29	MRSA	60690/60691
(1)	–	–	–	~	12500	12500	25000
(5)	–	–	100000	–	–	–	50000
(6)	3125	12500	–	6250	12500	6250	12500
(7)	781	6250	100000	100000	3125	3125	6250
(9)	781	–	–	–	–	–	–
(10)	6250	12500	–	25000	–	50000	–
Streptomycin	–	–	–	49	49	12	12
Nystatin	3125	3125	6250	–	–	–	–

Notes: – = Tested compound inactive, ~ = not tested.

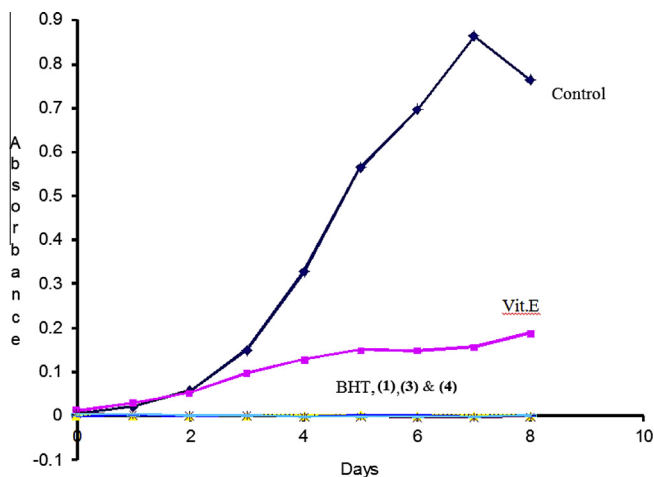


Fig. 6. Absorbance values of the compounds using FTC method.

C.A. Chelation by copper(II) ion enhances activity but chelation by nickel(II) ion generally reduces activity as was also observed by Akbar Ali et al. [9]. Complexation with cadmium(II) ion resulted in great enhancement of biological activity.

3.9. Antioxidant activities

The daily absorbance readings for (1), (3), (4), Vitamin E, BHT and the control solution are plotted in Fig. 6. (1), (3) and (4) show high antioxidant activity compared to Vitamin E, comparable to the commercially available BHT. The high antioxidant properties can be related to the presence of nitrogen or oxygen, which are active electron pair donors that can form coordination bonds but do not undergo ionization. Metal complexes were not tested using antioxidant assay because of their insolubility in the ethanolic medium.

4. Conclusion

In summary, this research has shown, relative to (1), the enhancement of cytotoxic activity upon the introduction of a pyridine ring, while the introduction of a benzoic acid group resulted in lower cytotoxic activity which might indicate that the pyridine ring acts as a pharmacophore. However, antimicrobial bioassay revealed different results whereby, relative to (1), activity was lowered by both Schiff base ligands. Results have highlighted the enhancement of bioactivity by chelation, specifically the high antifungal activity of (9) which would require further testing to ensure its high activity. Finally, this research emphasizes the interesting potential role of derivatives of (1) as antioxidants.

Acknowledgements

The authors thank the Ministry of Higher Education Malaysia (MOHE) under FRGS (F0010.54.02) for providing a grant for this

study. Khoo Teng Jin would like to extend his sincere gratitude to A. R. Cowley and D. J. Watkin in Crystallographic Research Laboratory, University of Oxford for their professional guidance and MOS-TI for the National Science Foundation (NSF) Scholarship and attachment grant.

Appendix A. Supplementary material

CCDC 294222 and 786894 contains the supplementary crystallographic data for this paper. These data can be obtained free of charge from The Cambridge Crystallographic Data Centre via www.ccdc.cam.ac.uk/data_request/cif. Supplementary data associated with this article can be found, in the online version, at <http://dx.doi.org/10.1016/j.ica.2014.01.001>.

References

- [1] N. Bharti, R. Maurya, F. Naqvi, A. Bhattacharya, S. Bhattacharya, A. Amir, *Eur. J. Med. Chem.* 35 (2000) 481.
- [2] J. Li, L. Zheng, I. King, W. Terrence, S. Chen, *Curr. Med. Chem.* 8 (2001) 121.
- [3] M. Ali, A. Mirza, R. Butcher, M. Tarafder, B. Tan, A. Ali, *J. Inorg. Biochem.* 92 (2002) 141.
- [4] M. Ali, R. Bose, *J. Inorg. Nucl. Chem.* 39 (1977) 265.
- [5] M. Ali, S. Livingstone, *Coord. Chem. Rev.* 13 (1974) 101.
- [6] M. Ali, M. Tarafder, *J. Inorg. Nucl. Chem.* 39 (1977) 1785.
- [7] M. Ali, C. Haroon, M. Nazimuddin, S. Majumder, M. Tarafder, M. Khair, *Transition Met. Chem.* 17 (1992) 133.
- [8] M. Tarafder, M. Ali, N. Saravanan, W. Weng, S. Kumar, N. Umar-Tsafe, K. Crouse, *Transition Met. Chem.* 25 (2000) 295.
- [9] M. Ali, K. Fernando, D. Palit, M. Nazimuddin, *Transition Met. Chem.* 20 (1995) 19.
- [10] S. Raj, B. Yamin, Y. Yusoff, M. Tarafder, H.-K. Fun, K. Crouse, *Acta Crystallogr., Sect. C* 56 (2000) 1236.
- [11] M. Tarafder, A. Kasbollah, K. Crouse, A. Ali, B. Yamin, H.-K. Fun, *Polyhedron* 20 (2001) 2363.
- [12] M. Tarafder, T.-J. Khoo, K. Crouse, A. Ali, B. Yamin, H.-K. Fun, *Polyhedron* 21 (2002) 2547.
- [13] M. Tarafder, T.-J. Khoo, K. Crouse, A. Ali, B. Yamin, H.-K. Fun, *Polyhedron* 21 (2002) 2691.
- [14] M. Hossain, M. Alam, J. Begum, M. Ali, M. Nazimuddin, F. Smith, R. Hynes, *Inorg. Chim. Acta* 249 (1996) 207.
- [15] K. Crouse, K.-B. Chew, M. Tarafder, A. Kasbollah, A. Ali, B. Yamin, H.-K. Fun, *Polyhedron* 23 (2004) 161.
- [16] Z. Otwinowski, W. Minor, in: C. Carter, R.M. Sweet (Eds.), *Processing of X-ray Diffraction Data Collected in Oscillation Mode*, Methods Enzymology, Academic Press, 1997, 276.
- [17] A. Altomare, G. Cascarano, G. Giacovazzo, A. Guagliardi, M. Burla, G. Polidori, M. Camalli, *J. Appl. Crystallogr.* 27 (1994) 435.
- [18] D. Watkin, C. Prout, J. Carruthers, P. Betteridge, R. Cooper, *J. Appl. Crystallogr.* 36 (2003) 1487.
- [19] T. Mosmann, *J. Immunol. Meth.* 65 (1983) 55.
- [20] C. Hufford, A. Clark, *Discovery and Development of New Drugs for Systemic Opportunistic Infections*, Studies in Natural Product Chemistry, vol. 2, Elsevier, Amsterdam, 1988, p. 421.
- [21] H. Kikuzaki, N. Nakatani, *J. Food Sci.* 58 (1993) 1407.
- [22] S. Karaböcek, N. Karaböcek, *Polyhedron* 16 (1997) 1771.
- [23] N. Raman, S. Ravichandran, C. Thangaraja, *J. Chem. Sci.* 116 (2004) 215.
- [24] E. Barefield, D. Busch, S. Nelson, *Q. Rev. Chem. Soc.* 22 (1968) 457.
- [25] M. Chapman, P. Ayyappan, B. Foxman, G. Yee, W. Lin, *Cryst. Growth Des.* 1 (2001) 159.
- [26] M. Kato, H. Jonassen, J. Fanning, *Chem. Rev.* 64 (1964) 99.
- [27] N. Halim, K. Kassim, A. Fadzil, B. Yamin, *Malays. J. Anal. Sci.* 16 (2012) 56.
- [28] T.-J. Khoo, M. Break, M. Tahir, K. Krouse, A. Cowley, D. Watkin, *Acta Crystallogr., Sect. E* 69 (2013) m323.
- [29] M. Break, S. Mehta, M. Tahir, K. Crouse, T.-J. Khoo, *Acta Crystallogr. Sect. E* 69 (2013) 178.